molecular pharmaceutics

pubs.acs.org/molecularpharmaceutics

Article

Targeted Delivery of Anti-inflammatory and Imaging Agents to Microglial Cells with Polymeric Nanoparticles

Celina Cahalane, Jason Bonezzi, John Shelestak, Robert Clements, Aliaksei Boika, Yang H. Yun,* and Leah P. Shriver*

Cite This: *Mol. Pharmaceutics* 2020, 17, 1816−1826

Read Online

ACCESS | Metrics & More | Article Recommendations | Supporting Information

ABSTRACT: Insult to the central nervous system (CNS) results in an early inflammatory response, which can be exploited as an initial indicator of neurological dysfunction. Nanoparticle drug delivery systems provide a mechanism to increase the uptake of drugs into specific cell types in the CNS such as microglia, the resident macrophage responsible for innate immune response. In this study, we developed two nanoparticle-based carriers as potential theranostic systems for drug delivery to microglial cells. Poly(lactic-*co*-glycolic) acid (PLGA)- and L-tyrosine polyphosphate (LTP)-based nanoparticles were synthesized to encapsulate the magnetic resonance imaging (MRI) contrast agent, gadolinium-diethylenetriaminepentaacetic acid (Gd[DTPA]), or the anti-inflammatory drug, rolipram. Robust uptake of both polymer formulations by microglial cells was observed with no evidence of toxicity. In mixed glial cultures, we observed a preferential internalization of nanoparticles by microglia compared to that of astrocytes. Moreover, exposure of our nanoparticles to microglial cells did not induce the release of the proinflammatory cytokines, tumor necrosis factor α (TNF-α), interleukin-1 β (IL-1β), or interleukin-6 (IL-6). These studies provide a foundation for the development of LTP nanoparticles as a platform for the delivery of imaging agents and drugs to the sites of neuroinflammation.

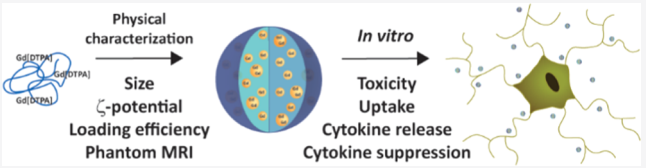

KEYWORDS: *nanoparticles, l-tyrosine polyphosphate, microglia, theranostic*

INTRODUCTION

Microglial cells are a component of the innate immune system within the central nervous system (CNS) that serve as sentinels for the detection of infection,[1] secrete factors involved in modulating immune responses,[2] and enhance tissue repair.[3] However, during chronic inflammation, activated microglial cells can also participate in tissue destruction through antigen presentation and the release of proinflammatory factors such as IL-1β and NO.[4−7] In addition, microglial cells become activated early in the disease process, often before the appearance of adaptive immune cells, suggesting a central role for these cells in mediating pro- versus anti-inflammatory effects.[8,9]

Cyclic nucleotides, cyclic adenosine 3′,5′-monophosphate (cAMP), and cyclic guanosine 3′,5′-monophosphate (cGMP) are second messengers involved in central nervous system and immune cell responses.[10] These molecules are produced by the action of adenylyl cyclases and guanylyl cyclases, and their signaling activity is stopped through their hydrolysis to inactive AMP or GMP via phosphodiesterases (PDEs).[11] PDEs are categorized into 11 families (PDE1-11) with different substrate specificities and physiological roles.[12] PDE4 degrades cAMP and plays a primary role in mediating the release of inflammatory molecules from immune cells. Within microglial cells, the control of cAMP levels through multiple PDE4 isoforms regulates cell responses to inflammatory mediators,[13] signaling,[14] and cytokine production.[15] Conversely, the inhibition of phosphodiesterase activity reduces symptoms in models of neuroinflammation.[16] The clinical development of PDE4 inhibitors has been prevented by the side effects of nausea and emesis.[17] However, new formulations that prevent these symptoms may open this class of drugs to further testing.

Magnetic resonance imaging (MRI) is used clinically to detect lesions within the brain and spinal cord. MRI can be performed with or without the addition of a gadolinium-based contrast agent. Gadolinium (Gd) is paramagnetic and shortens the T_1 relaxation times of hydrogens in neighboring water molecules, giving bright contrast on T_1 images. Gadolinium has a similar ionic radius to calcium and has the potential to inhibit calcium-dependent processing;[18,19] therefore, contrast agents utilize both linear and macrocyclic ligands such as diethylenetriaminepentaacetic acid (DTPA) or 1,4,7,10-tetraazacyclododecane-1,4,7,10-tetraacetic acid (DOTA). These agents primarily detect blood−brain barrier breakdown; however, they do not provide cellular resolution, which limits the ability to distinguish pathologies.[20] The encapsulation of gadolinium within nano-

Received: May 5, 2019
Revised: March 19, 2020
Accepted: March 26, 2020
Published: March 26, 2020

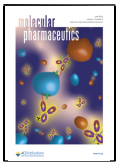

https://dx.doi.org/10.1021/acs.molpharmaceut.9b00489
Mol. Pharmaceutics 2020, 17, 1816−1826

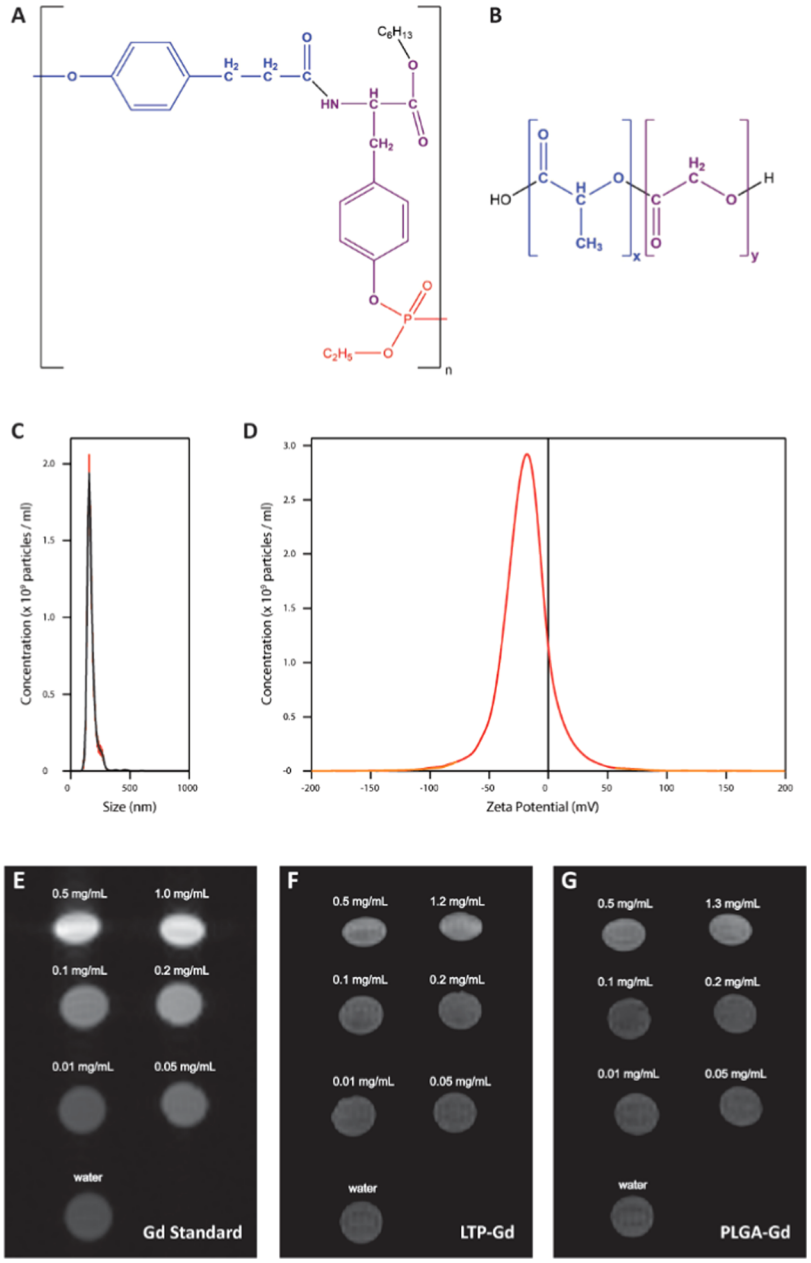

Figure 1. Nanoparticle characterization. (A) LTP repeat unit consists of the L-dopa derivative desaminotyrosine (blue), L-tyrosine (violet) with protecting hexyl group on the carboxy terminus (black), and phosphate (red). (B) PLGA repeat unit consists of lactic acid (blue) and glycolic acid (violet). (C) Size distribution and (D) ζ-potential measurements of blank LTP nanoparticle suspensions (400 μg/mL) by dynamic light scattering. T_1-weighted phantom MRI images of (E) Gd[DTPA] standards versus (F) LTP-Gd or (G) PLGA-Gd.

particle formulations is one avenue of research to overcome this problem, as well as issues with gadolinium toxicity. Current preclinical formulations of gadolinium include branched polyethyleneimine particles conjugated to gadolinium DTPA,[21] gold nanoshells coated with BSA-Gd,[22] gadolinium-polydopamine nanoparticles,[23] and others.[24,25] The nanoparticle-based formulations containing gadolinium would allow the direct targeting of agent to sites of disease, increasing resolution and reducing toxicity. However, tissue-specific uptake will require specific targeting ligands, and adequate biodistribution of particles remains challenging.

Here, we have developed two nanoparticle-based theranostics in a proof-of-principle study. Both formulations consist of nanoparticles that encapsulate either gadolinium and the PDE4 inhibitor, rolipram, in L-tyrosine polyphosphate (LTP) or poly(lactic-*co*-glycolic) acid (PLGA) polymers (Figure 1). LTP nanoparticles were first described by Ditto et al. as a potential controlled-release intracellular delivery system.[26,27] Unlike most polymer-based biodegradable nanoparticles, including PLGA, LTP-based nanoparticles were found to degrade within days as opposed to months.[28−30] The backbone of LTP and PLGA is modifiable, and both polymers are biocompatible materials that have been previously tested for the delivery of therapeutics such as DNA and small molecule drugs.[31−33] We demonstrate that these nanoparticle formulations are rapidly taken up by microglial cells and do not induce inflammatory activation of these cells. A theranostic that incorporates rolipram and gadolinium may also allow targeting of the initial stages of neuroinflammation.

https://dx.doi.org/10.1021/acs.molpharmaceut.9b00489
Mol. Pharmaceutics 2020, 17, 1816−1826

MATERIALS AND METHODS

Chemicals. Gd[DTPA] (diethylenetriaminepentaacetic acid gadolinium (III) dihydrogen salt hydrate) was purchased from Sigma-Aldrich (St. Louis, MO) and dissolved in deionized water (DI-H_2O) at 37 °C at a concentration of 5.0 mg/mL. A stock solution of rolipram (Enzo Life Sciences, Farmingdale, NY, BML-PD175-0010, ≥98%) was dissolved in ethanol (EtOH) at 37 °C at a concentration of 1.0 mg/mL. Certified reference gadolinium standard for ICP was purchased from VWR (82025-986). Poly(lactic-*co*-glycolic acid) (PLGA, Lakeshore Biomaterials, Birmingham, AL, 5050 DLG1A, MW of 4200 Da) was dissolved in chloroform at room temperature. Linear polyethyleneimine (LPEI, 25 KDa) was obtained from PolyScience Inc. and dissolved in DI-H_2O at a concentration of 11 mg/mL. Poly(ethylene glycol) grafted to chitosan (Carbomer Inc., San Diego, CA, PEG-g-CHN) was dissolved in 0.1 N acetic acid (3.3 mg/mL). A 5% (w/v) solution of poly(vinylpyrrolidone) (PVP, Alfa Aesar, Tewksbury, MA, 8 KDa) was made in DI-H_2O. Bovine serum albumin-fluorescein isothiocyanate (BSA-FITC) was purchased from Fisher Scientific and dissolved in DI-H_2O (3% w/v). LC−MS-grade acetonitrile (ACN), methanol (MeOH), chloroform ($CHCl_3$), and water were obtained from Fisher Scientific (Waltham, MA).

Nanoparticles. The LTP polymer was synthesized using a previously developed protocol.[34] Both LTP and PLGA nanoparticles were prepared by a water-in-oil-in-water emulsion and solvent evaporation technique described previously.[35] Four formulations, blank (unloaded), FITC-loaded, Gd[DTPA]-loaded, and rolipram-loaded LTP nanoparticles, were synthesized as follows: 194 mg LTP in 6 mL of chloroform, 0.67 mL of 3.0 mg/mL LPEI, 0.61 mL of 3.3 mg/mL PEG-g-CHN, and either 3% BSA-FITC, 1% rolipram, or 1% Gd[DTPA] (w/w) were added to a 250 mL round-bottom flask. This mixture formed the initial emulsion using a high-speed stirrer (Yamato Lab-Stirrer LR400D) at 2000 rpm for 1 min. Afterward, 92 mL of 5% PVP was added and vortexed at 1600 rpm for 3 min to form the final emulsion. The chloroform was then allowed to evaporate overnight with gentle stirring. Nanoparticles were then washed twice with DI-H_2O and centrifuged for 20 min at 15 000*g*. Finally, the nanoparticle formulations were shell-frozen in 10 mL of DI-H_2O, lyophilized for 72 h, and then stored in a desiccator until usage.

PLGA nanoparticle synthesis was performed using the above method with the exception of substituting PLGA for LTP and adding 5% Gd[DTPA] instead of 1%.

Cell Culture. The mouse microglial cell line, SIM-A9, was purchased from ATCC (CRL-3265). Cells were cultured and maintained in growth media consisting of Dulbecco's modified Eagle's medium, Ham's F-12 50/50 Mix (DMEM/F-12 50/50, 1×) with 10% fetal bovine serum (FBS), 5% horse serum (HS), and 1% penicillin/streptomycin (P/S) at 37 °C and 5% CO_2.

All animal studies were approved by the IACUC of the University of Akron and performed in accordance with the Public Health Service procedures and Animal Welfare Act guidelines. Primary mixed glia were harvested from the cerebral cortices of 1 day postnatal CD-1 mice. Mixed cultures were maintained in growth media (-HS) at 37 °C and 5% CO_2 until ∼90% confluent (approximately 12−15 days). Confluent mixed glial cultures were used to isolate primary microglial cells following the protocol established by Saura et al.[36] Briefly, mixed glial cultures were plated according to the specific experiment. Cells were incubated for 24 h at 37 °C and 5% CO_2 to allow cells to adhere. The following day, cells were washed with growth media without serum (-FBS, -HS) and then treated with 1:3 of 0.25% trypsin, 2.21 mM EDTA, and 1×: growth media (-FBS, -HS) and incubated at 37 °C and 5% CO_2 for up to 2 h depending on the well size. Once the upper layer of cells was completely detached from the well, the process was deactivated by the addition of excess growth media with FBS. The media containing the detached layer of astrocytes and oligodendrocytes was removed and replaced with fresh growth media (-HS). Microglia remained attached to the well.

Size Distribution and ζ-Potential. Each formulation of LTP nanoparticles (blank -Gd, -Rol) was analyzed by dynamic light scattering for size and aggregation potential. Suspensions of nanoparticles in DI-H_2O were prepared at 400 μg/mL and flowed through a Nanosight NS500 (Malvern Panalytical, Westborough, MA). Camera brightness and focus were manually adjusted for measurement optimization. Size distribution measurements were performed 5 times for each sample with a 60 s capture duration for each measurement. ζ-potential measurements were optimized at 24 V. Measurements were repeated twice for each sample with a 30 s capture duration for each measurement. Data were analyzed using NTS 3.1 software.

Loading Efficiency. The loading efficiencies of both LTP and PLGA nanoparticles with Gd[DTPA] were determined using an Agilent 700 Series inductively coupled plasma-optical emission spectrometer (ICP-OES) (Agilent, Santa Clara, CA). 1.8 mg LTP-Gd or 1.5 mg PLGA-Gd was resuspended in 1.5 mL of DI-H_2O and digested in 0.2 mL HNO_3 and 0.5 mL HCl. The digest was then brought up to 5 mL total volume with DI-H_2O. The concentration of Gd was determined against a gadolinium standard prepared in 0.6 M HCl/0.3 M HNO_3 at 0.05, 0.5, and 2.5 mg/mL.

MRI. Gadolinium-loaded nanoparticles were imaged by T_1-weighted MRI for contrast enhancement potential. Suspensions of either LTP-Gd or PLGA-Gd nanoparticles were prepared in DI-H_2O by dilution from primary stocks at 1.2 mg/mL (LTP-Gd) and 1.3 mg/mL (PLGA-Gd) in DI-H_2O. Decreasing concentrations at 0.5, 0.2, 0.1, 0.05, and 0.01 mg/mL were prepared for both nanoparticle types. Standard solutions of Gd[DTPA] in DI-H_2O were also prepared at the same concentrations, with the exception to the highest standard at 1.0 mg/mL.

Nanoparticles were imaged using a Bruker Icon 1T-magnetic resonance imaging system (Bruker, Billerica, MA). Cross-sectional T_1 fast low-angle shot (FLASH) slices were taken to measure MR signal intensity. The nanoparticle preparations were arrayed in ascending concentrations from DI-H_2O to 1 mg/mL. T_1 FLASH images of the solutions were acquired with a field of view (FOV) of 60 × 60 mm^2 over a 128 × 128 matrix. Transverse slices (0.750 mm thick) were taken with an echo time (TE) of 10 ms and a repetition time (TR) of 250 ms. Similar images of smaller sets of nanoparticle dilutions were taken against common gadolinium contrast agents to compare the contrast intensity using identical image settings. Data were saved in the dicom format and analyzed using ImageJ.[37]

Cell Viability. The viability of SIM-A9 cells and primary microglia after exposure to the nanoparticle formulations was determined using a resazurin-based viability kit (TOX-8, Sigma-Aldrich, St. Louis, MO). Cells were plated at approximately 1 × 10^5 cells/well and allowed to adhere overnight. Cells were then treated with blank, -Gd, or -Rol formulations of LTP- and PLGA-based nanoparticles at 50, 100, 200, and 500 μg/mL in phosphate-buffered saline (PBS) for 24 h. PBS alone and H_2O_2

https://dx.doi.org/10.1021/acs.molpharmaceut.9b00489
Mol. Pharmaceutics 2020, 17, 1816−1826

or 30% EthOH were used as controls (n = 10 in SIM-A9, n = 6 in primary microglia for each treatment type). Resazurin solution was added to each well at 10% of media volume and allowed to incubate at 37 °C for 3 h prior to analysis. Fluorometric analysis was performed on a SpectraMax M2*e* (Molecular Devices, San Jose, CA) microplate reader with an excitation wavelength of 560 nm and an emission wavelength of 590 nm.

Metabolomics. Metabolic changes occurring in SIM-A9 cells and primary microglia after exposure to either PLGA-blank or LTP-blank nanoparticles were monitored by liquid chromatography−mass spectrometry (LC−MS). Cells were plated in 6-well plates at approximately 1×10^6 cells per well and allowed to adhere overnight. Cells were then treated with PBS vehicle or 100 μg/mL of LTP-blank or PLGA-blank nanoparticles for 24 h (n = 3 for each group for primary microglia, n = 6 for each group for SIM-A9 cells).

After treatment, polar metabolites were extracted from the lysed cells using a protocol modified from Bligh and Dyer.[38] Briefly, cells were scraped from the bottom of the wells with a mixture of 10% methanol (MeOH). The cell lysate was then subjected to three rounds of vortex−freeze−thaw followed by sonication. A mixture of $CHCl_3$/MeOH 1:2 (v/v) was added followed by H_2O and then vortexed and placed at −20 °C for 1 h. Samples were then centrifuged to allow separation of aqueous and organic phases. The upper, aqueous phase containing the polar metabolites was recovered, dried to residue by centrivap, and then reconstituted in 100 μL of 70% ACN.

Polar metabolites were separated on an Eksigent Micro200LC (ABSciex, Framingham, MA) by hydrophilic interaction liquid chromatography (HILIC) (Luna 3 μm NH_2, 150 × 1 mm^2, 100 Å, Phenomenex). Five microliters of sample was injected into the instrument. Mobile phase A consisted of water and 5 mM ammonium acetate. Mobile phase B consisted of acetonitrile with 5 mM ammonium acetate. The chromatographic method followed a gradient elution at 30 μL/min with the following conditions: 0−1 min 95% B, 1−5 min 80% B, 5−6 min 46% B, 6−13 min 14.7% B, 13−14 min 0% B, 14−17 min 0% B, 17−17.1 min 95% B, 17−25 min 95% B. Metabolites were analyzed in positive mode with a TripleTOF 5600+ mass spectrometer (ABSciex, Framingham, MA) with the following parameters: 15 psi nebulizer gas, 20 psi heater gas, ion spray voltage 5000 eV, declustering potential 100 eV, TOF MS scan 60−1000 Da, fragmentation collision spread 25−40 eV. Data was acquired by information-dependent acquisition (IDA).

Immunofluorescence Evaluation of Cellular Uptake. Cells were plated in 6-well plates containing poly-L-lysine-coated coverslips at approximately 1×10^6 cells/well and allowed to adhere overnight. Cells were treated with 100 μg/mL of either LTP-FITC or PLGA-FITC nanoparticles for 24 h. After treatment, cells were fixed with 4% paraformaldehyde and blocked with 10% FBS prior to antibody treatment. For primary mixed cultures, cells were permeabilized with 0.2% Triton X-100 after fixing and prior to blocking. SIM-A9 and primary microglia were probed with anti-F4/80 conjugated to eFluor570 (eBioscience, Waltham, MA). Primary astrocytes were probed with anti-GFAP conjugated to eFluor660 (eBioscience, cat#50-9892-82, 1:80). DAPI was used as a nuclear stain (Sigma-Aldrich, cat #D9542). Images were taken using a Nikon A1 confocal microscope at a 60× magnification.

Cytokine Release and Deactivation. SIM-A9 and primary microglia were tested for release of the inflammatory cytokines tumor necrosis factor α (TNF-α), IL-1β (interleukin-1β), and IL-6 (interleukin-6), as well as LTP- or PLGA-Rol suppression of the cytokines using the multiplexing MAGPIX system (MilliporeSigma, Billerica, MA) and a customized magnetic bead panel. Cells were plated at 1×10^5 cells per well and allowed to adhere overnight. Lipopolysaccharide (LPS) (Sigma-Aldrich, St. Louis, MO) at 1, 10, and 100 ng/mL was used as a positive control. Cells were treated with 100 μg/mL of -Rol nanoparticle formulations (LTP or PLGA) for 24 h prior to harvesting media. Cells were also treated with both LPS (1 ng/mL, 10 ng/mL, or 100 ng/mL) and LTP-Rol or PLGA-Rol (100 μg/mL for both formulations) to determine the release of drug for anti-inflammatory action (n = 3 for each group). Media was immediately stored at −80 °C until analysis.

Statistical Analysis. Analysis of variation (ANOVA) was performed using Prism 8 software (GraphPad Software, San Diego, CA). Comparison between control and experimental groups was assessed by Tukey's test for multiple comparisons (one-way ANOVA; cytokine assay) or Sidak's correction for multiple comparison testing (two-way ANOVA; viability assay) with a family-wise significance value of 0.05 and a 95% confidence interval.[39] Results of $p \leq 0.05$ were considered significant. Principal component analysis (PCA) was performed using Scaffold Elements software v.1.4.0 (Proteome Software, Portland, OR).

RESULTS

Characterization of Nanoparticle Formulations. The structure of the LTP monomer consists of desaminotyrosine (blue) and L-tyrosine (violet) linked through an enzyme degradable peptide bond (Figure 1A). The polyamino acid structure modifications also result in bioavailable alcohols and phosphate that do not affect cellular pH.[40] Although PLGA has been a highly studied polymer for use in nanoparticle applications,[41] the repeat unit of PLGA (Figure 1B) consists of lactic (blue) and glycolic (violet) acids, which have been found to decrease local pH upon degradation resulting in an inflammatory response in bone fracture fixation applications.[42] Our study aimed to compare the effectiveness of LTP nanoparticles with that of PLGA to determine its feasibility as a theranostic delivery system to the CNS.

We first determined the size and ζ-potential of the different nanoparticle formulations by monitoring the light scattering and Brownian motion of nanoparticle suspensions in water (Figure 1, Supporting Information, Figure 1). The blank LTP formulation was found to have a mean particle size of 178.0 ± 0.5 nm (Figure 1C), coinciding with the size determination made when LTP nanoparticles were originally characterized.[26] Gd[DTPA]- and rolipram-loaded LTP suspensions had mean sizes of 269.2 ± 5.4 and 273.3 ± 7.7 nm, respectively (Supporting Information, Figure 1A,C), with the loaded compounds expectantly owing to the slight size increase. ζ-Potential measurements for LTP-blank, -Gd, and -Rol formulations resulted in mean values of −38.8, −29.3, and −32.7 mV, respectively (Figure 1D, Supporting Information, Figure 1B,D). The similarities between the ζ-potential values for the different formulations suggest that the encapsulation process does not affect surface potential. We next determined the loading efficiency of Gd[DTPA] into LTP and PLGA nanoparticles by ICP-OES. The intensity of emission was monitored at 335 nm and compared against a Gd standard curve (0.005−2.5 mg/L) (Supporting Information, Figure 2). Loading was determined by calculating the amount of Gd (in mg) per mg nanoparticle. The resulting values were 0.043 mg/L for LTP-Gd and 0.15 mg/L for PLGA-Gd, corresponding to a

https://dx.doi.org/10.1021/acs.molpharmaceut.9b00489
Mol. Pharmaceutics 2020, 17, 1816−1826

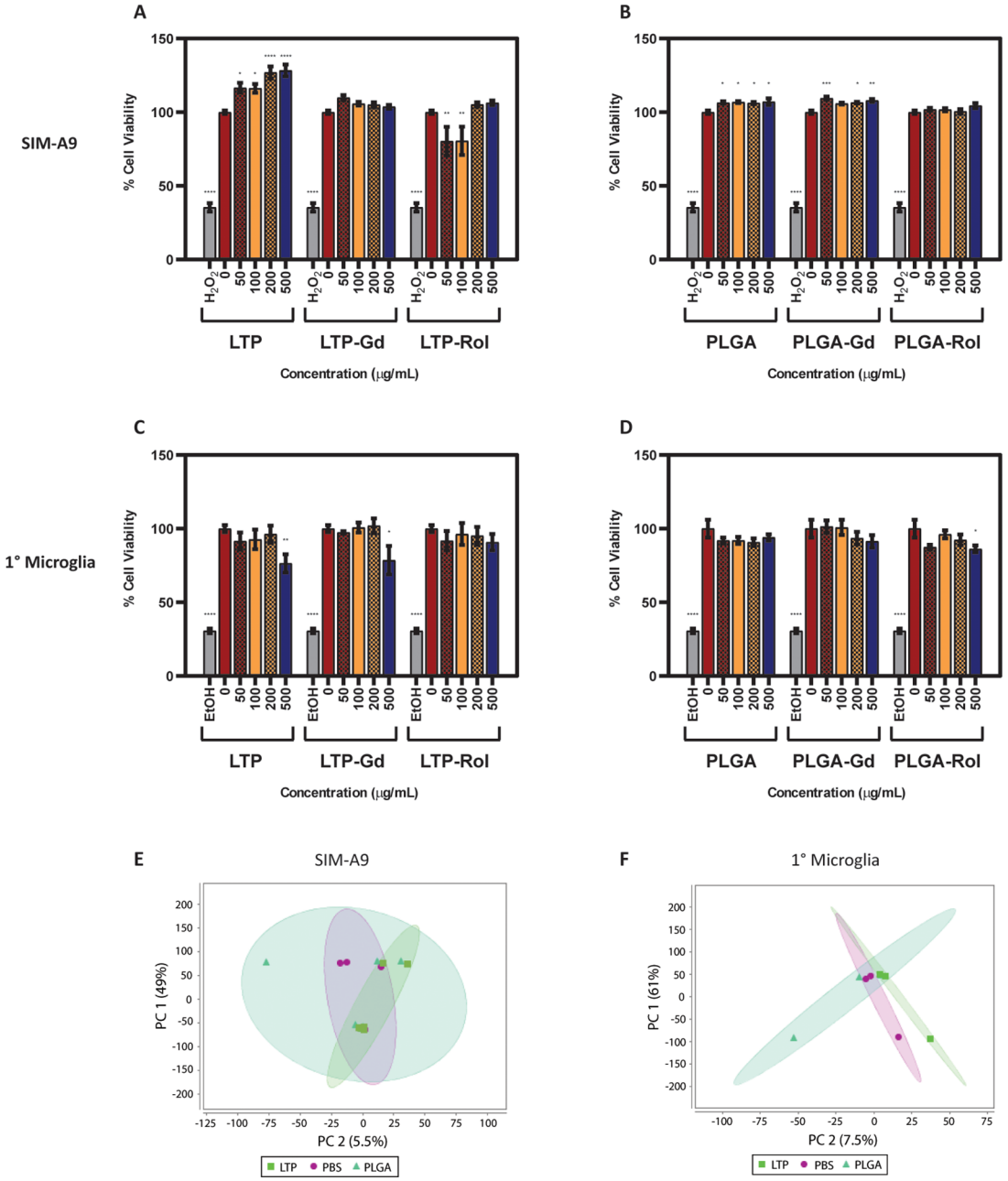

Figure 2. Nanoparticle formulations are nontoxic to microglial cells. SIM-A9 cells were treated with (A) LTP or (B) PLGA nanoparticle formulations at various concentrations for 24 h and compared to PBS as a positive control. Thirty percent of H_2O_2 was used as a negative control (n = 10 in each group). Primary microglia were exposed to (C) LTP or (D) PLGA formulations at similar concentrations for 24 h. Thirty percent of EtOH was used as a negative control (n = 6 in each group). All data expressed as mean ± SEM; $^*p \leq 0.05$, $^{**}p \leq 0.01$, $^{***}p \leq 0.001$, $^{****}p \leq 0.0001$ versus positive control group. PCA plots of SIM-A9 (E) and primary microglia (F) show no metabolic variation between LTP-blank, PLGA-blank, or PBS-treated groups after 24 h treatment (n = 6 for each SIM-A9 group; n = 3 for each primary microglia group). Ellipses show 95% confidence interval.

1.2% (w/w) loading of Gd in LTP and 0.98% (w/w) loading of Gd in PLGA nanoparticles (Supporting Information, Table 1). MRI phantom imaging was used to determine if the amount of Gd[DTPA] loaded into the nanoparticles was sufficient for contrast enhancement in both LTP and PLGA formulations compared to Gd[DTPA] standards (Figure 1). Increasing positive image contrast can be seen with increasing concentration for both LTP-Gd (Figure 1F) and PLGA-Gd (Figure 1G) formulations compared to water. Moreover, the degree of enhancement increases similarly in both formulations. However, the highest concentration suspensions (1.2 mg/mL LTP-Gd, 1.3 mg/mL PLGA-Gd) show enhancement intensities comparable to the 0.1 mg/mL Gd[DTPA] standard (Figure 1E).

The translational potential of our nanoparticles was determined by examining the toxicity of our formulations in microglial cells. We treated the SIM-A9 microglial cell line and primary microglia isolated from mice with either LTP or PLGA nanoparticles that were loaded with rolipram or Gd[DTPA] at concentrations that ranged from 50 to 500 μg/mL. For both SIM-A9 and primary microglial cells, exposure to blank, -Gd, or -Rol formulations of either LTP or PLGA did not decrease viability after 24 hours of incubation (Figure 2). SIM-A9 cells show greater than 80% viability compared to positive controls

https://dx.doi.org/10.1021/acs.molpharmaceut.9b00489
Mol. Pharmaceutics 2020, 17, 1816−1826

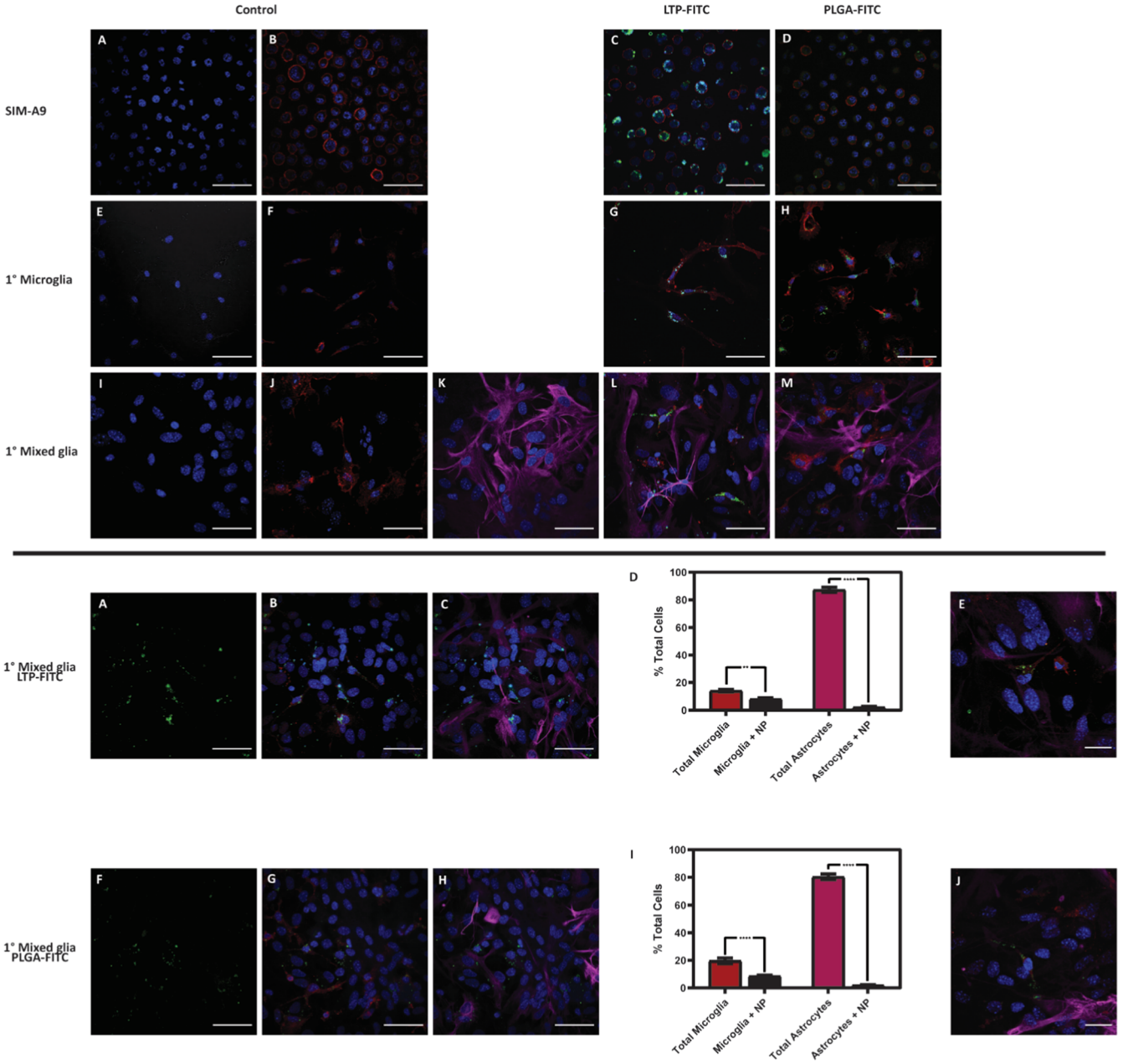

Figure 3. Nanoparticles are preferentially taken up by microglia. Top panel: confocal images show the uptake of (C) LTP-FITC and (D) PLGA-FITC nanoparticles at 100 μg/mL and 24 h exposure by SIM-A9 cells. (E−H) Isolated primary microglia also show a positive uptake of both (G) LTP-FITC and (H) PLGA-FITC nanoparticles at 100 μg/mL and 24 h. (I−M) Microglia show an efficient uptake of both (L) LTP-FITC and (M) PLGA-FITC at 100 μg/mL and 24 h treatment compared to astrocytes in primary mixed glial cultures. Bottom panel: LTP-FITC nanoparticles (A) and PLGA nanoparticles (F) are preferentially taken up by microglia (B: LTP-FITC) (G: PLGA-FITC) compared to astrocytes (C: LTP-FITC) (H: PLGA-FITC) in mixed glial cultures. (D: I) Microglia make up ≈20% of the total cells in mixed glial culture, and astrocytes make up ≈80% of total cells. For both LTP-FITC and PLGA-FITC nanoparticles, ≈50% of total microglia show nanoparticle uptake, while astrocytes show ≈ 2.5% association with nanoparticles. Data expressed as mean ± SEM; $^{**}p \leq 0.01$, $^{****}p \leq 0.0001$ versus total cells. Magnification = 60×. Scale bars represent 50 μm. (E: LTP-FITC) (J: PLGA-FITC) 100× magnification showing microglial uptake of nanoparticles in mixed glial culture. Scale bars represent 20 μm. (blue = DAPI, nucleus; red = anti-F4/80, microglia; green = FITC, nanoparticles; magenta = anti-GFAP, astrocytes).

(PBS, 0 μg/mL) when exposed to all LTP formulations and concentrations (Figure 2A). When treated with all PLGA formulations and concentrations, viability was shown at or near 100% compared to positive controls (Figure 2B). Similarly, primary microglia exposed to all LTP formulations and concentrations show greater than 80% viability when compared to positive controls (Figure 2C). Likewise, exposure to all PLGA formulations and concentrations shows closer to 100% viability for primary microglia (Figure 2D).

Global metabolic profiling was performed on both SIM-A9 cells and primary microglia. Both cell types were treated with 100 μg/mL of either LTP-blank or PLGA-blank nanoparticles for 24 h prior to the extraction of polar metabolites and LC−MS analysis (Figure 2E,F). Multivariate statistical analysis was used to determine differences between the groups. The principal component analysis (PCA) plot shows that for SIM-A9 cells, treatment with either type of nanoparticle results in similar metabolic profiles between PBS-treated cells or nanoparticle-

https://dx.doi.org/10.1021/acs.molpharmaceut.9b00489
Mol. Pharmaceutics 2020, 17, 1816−1826

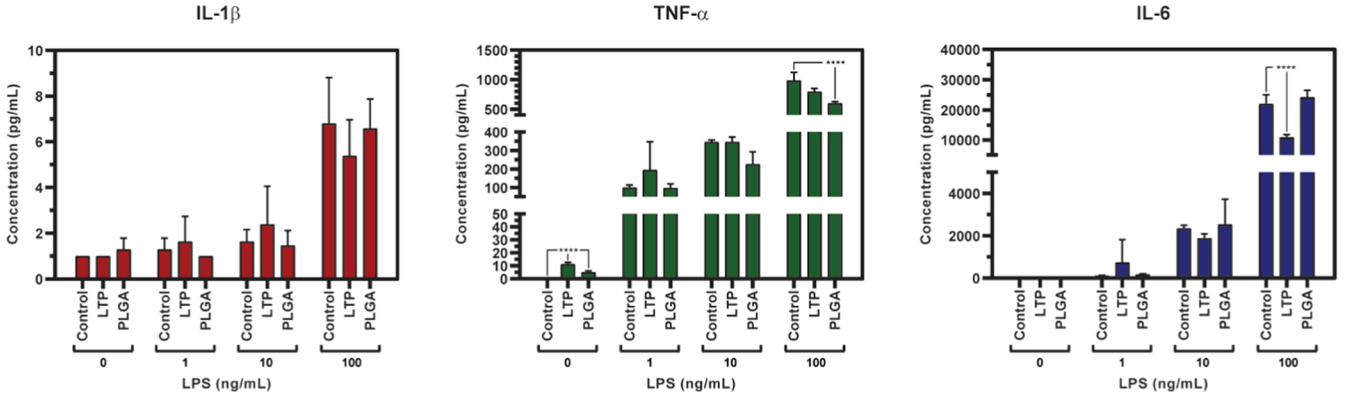

Figure 4. Nanoparticle uptake by microglial cells does not stimulate cytokine release. Release of proinflammatory cytokines IL-1β, TNF-α, and IL-6 by SIM-A9 cells was measured by multiplex technology. LPS at varying concentrations (1, 10, and 100 ng/mL) was used as a positive activator of cytokine release. Cells were treated with LTP-Rol (100 μg/mL) or PLGA-Rol (100 μg/mL) for 24 h prior to media harvest. Cells were also cotreated with varying concentrations of LPS (1, 10, and 100 ng/mL) and either LTP-Rol (100 μg/mL) or PLGA-Rol (100 μg/mL). LPS stimulation (all concentrations) does not induce IL-1β release, with or without cotreatment with nanoparticles. Cells show increasing TNF-α production with increasing LPS concentration. Cotreatment with 100 ng/mL LPS and 100 mg/mL PLGA-Rol nanoparticles shows a significant decrease in TNF-α production. Similarly, IL-6 production in SIM-A9 cells increases with increasing LPS concentration, with a significant decrease in IL-6 production in cells cotreated with 100 ng/mL LPS and 100 mg/mL LTP-Rol nanoparticles (n = 3 for each group). ****$p \leq 0.0001$ versus control.

treated cells (Figure 2E). Similar results are also seen in primary microglial cells treated with nanoparticles (Figure 2F).

Confocal microscopy was used to visualize the cellular uptake of both LTP- and PLGA-FITC-encapsulated nanoparticles (Figure 3). Cells were incubated with both FITC-loaded LTP and PLGA nanoparticle formulations for 24 h and subsequently stained with antibodies against F4/80 (microglia) or GFAP (astrocytes). Activation of microglial cells results in a shift from a ramified morphology toward an ameboid phenotype, and these alterations in cell shape would indicate the potential stimulation of immune surveillance activities by these cells after nanoparticle uptake.[43] Treatment of SIM-A9 (Figure 3A−D, top panel) or primary glial (Figure 3E−M, top panel) cultures with FITC-loaded PLGA or LTP nanoparticles did not induce such morphological changes in these cells. Twenty-four hours of exposure to either LTP-FITC (Figure 3C, top panel) or PLGA-FITC (Figure 3D, top panel) nanoparticles did not alter the morphology of the SIM-A9 cells as the primarily round shape seen in untreated SIM-A9 cells (Figure 3A,B, top panel) is maintained. Cellular processes are more distinctly observed in resting primary microglia (Figure 3E,F, top panel). Uptake of LTP-FITC nanoparticles does not appear to affect cell morphology (Figure 3G, top panel) in either cell type; however, microglia treated with PLGA-FITC nanoparticles (Figure 3H, top panel) showed some process retraction and an increase in cytosolic space around the nucleus.

Within the CNS, astrocytes could also take up nanoparticle formulations.[44] We further examined the uptake of our nanoparticles by microglia with respect to astrocytes in mixed glial cultures (Figure 3I−M, top panel; Figure 3A−J; bottom panel; Supporting Information, Figure 3A−H). Resting primary microglia (red) in mixed culture are characteristically small and thin with extended processes (Figure 3J, top panel) compared to the larger astrocytes (violet, Figure 3K, top panel). Treatment of mixed glial cultures with either LTP-FITC (Figure 3L, top panel; Figure 3A−E, bottom panel; Supporting Information, Figure 3A−D) or PLGA-FITC (Figure 3M, top panel; Figure 3F−J, bottom panel; Supporting Information, Figure 3E−H) shows no distinct alterations in microglial cell shape upon uptake. Moreover, astrocytes did not efficiently take up nanoparticles compared to microglial cells that contained nanoparticles surrounding the nuclei (Figure 3L,M, top panel; Figure 3A−J, bottom panel; Supporting Information, Figure 3). We subsequently quantified nanoparticle uptake in mixed glial cultures (Figure 3D,I, bottom panel). Approximately 20% of the total cell population in mixed cultures consists of microglia based on comparison of the fluorescence signals of anti-F4/80 (red) versus anti-GFAP (violet). Within the microglial population, LTP-FITC nanoparticles were taken up by 57.6% (Figure 3D, bottom panel), while PLGA-FITC nanoparticles were taken up by 44.1% (Figure 3I, bottom panel). In contrast, only 2.5 and 2.4% of astrocytes showed an uptake of LTP-FITC or PLGA-FITC nanoparticles, respectively (Figure 3D,I, bottom panel).

Inflammatory activation of microglia induces the release of multiple proinflammatory cytokines, most notably IL-6, IL-1β, and TNF-α, which have pleiotropic activity and have been associated with pathology in the CNS.[45,46] Cytokine release was monitored and quantified by multiplex technology to determine whether the nanoparticles alone induced the activation of microglial cells and if rolipram-loaded nanoparticles could inhibit cytokine release (Figure 4, Supporting Information, Figure 3). SIM-A9 cell stimulation with LPS at increasing concentrations (1−100 ng/mL) resulted in the increased secretion of TNF-α, IL-1β, and IL-6 after 24 h of treatment. Nanoparticle treatment alone in the absence of LPS stimulation did not result in cytokine release. LPS-stimulated cells were cotreated with 100 μg/mL of rolipram-loaded nanoparticles (LTP or PLGA formulations). At the highest dose of LPS (100 ng/mL), cotreatment with PLGA-Rol nanoparticles showed some suppression of TNF-α, which was not observed with LTP-Rol nanoparticles. Conversely, cotreatment at the highest concentration of LPS showed suppression of IL-6 by LTP-Rol nanoparticles but not PLGA nanoparticles. Neither formulation impacted IL-1β secretion at any concentration of LPS.

DISCUSSION

Polymer-based nanoparticles are of great interest as potential drug delivery systems. As technology has advanced, the push has been toward biodegradable and bioavailable degradation

https://dx.doi.org/10.1021/acs.molpharmaceut.9b00489
Mol. Pharmaceutics 2020, 17, 1816−1826

products to minimize adverse effects and maximize drug efficacy. Here, we introduce an alternative polymer formulation, LTP, with the potential to deliver diagnostic and therapeutic drugs for the detection and prevention of early neuroinflammation. This proof-of-concept study compares a novel biopolymer to the well-studied polymer PLGA system. Compared to PLGA, nanoparticles synthesized with LTP may allow for faster clearance and metabolism of less harmful byproducts, as well as a quicker release of drug payload.

Nanoparticle size plays an important role in cellular uptake, either by phagocytosis, receptor-mediated endocytosis, or pinocytosis.[47] Destache et al. characterized PLGA nanoparticles loaded with the antiretroviral drugs ritovanir, lopinavir, or efavirenz in peripheral blood mononuclear cells (PBMCs) and monocyte-derived macrophages (MDMs).[48] The study found the average size of drug-encapsulated PLGA nanoparticles to be 262 ± 83.9 nm and were readily taken up by MDMs as evidenced by fluorescence microscopy. We measured the size distribution of our various LTP nanoparticle formulations and found that the mean nanoparticle size varied from 178.0 to 273.3 nm, depending on formulation (Figure 1C, Supporting Information, Figure 1A,C). This size range was well within the limits recognized by microglia for endocytic internalization by either receptor-mediated endocytosis (RME)[49,50] or macropinocytosis.[51,52]

We further measured ζ-potential values as a means for determining nanoparticle stability in aqueous solutions. Lower magnitude ζ-potential values, regardless of sign (positive/negative), signify a higher probability for nanoparticle aggregation versus higher potential values.[53,54] However, due to the negative charge of cell membranes, values greater than +30 mV, while indicative of high stability (low tendency for aggregation), imply a cationic nanoparticle surface associated with increased cell membrane disruption.[55] Recent studies of PLGA nanoparticles for drug delivery have shown −6.63 and −14.25 mV ζ-potential values with minimal cell toxicity.[31,32] Our results show mean ζ-potential values of −38.8, −29.3, and −32.7 mV for blank LTP, -Gd, and -Rol formulations, respectively (Figure 1D, Supporting Information, Figure 1B,D). These results suggest an anionic nanoparticle surface with high stability in water. We were unable to obtain PLGA data as none of our formulations (blank, -Gd, -Rol) responded to the applied field voltage for size and ζ-potential analysis.

Gadolinium chelates exploit the paramagnetic character of Gd^{3+} to increase the longitudinal relaxivity (T_1) of protons on coordinated water molecules.[56,57] Chelating agents not only decrease the toxicity of the metal ion by preventing Ca^{2+} replacement but also increase the water molecule coordination time.[24] Challenges arise in fine tuning the exchange time of the metal−water complex to maximize T_1-weighted imaging.[58] Our phantom MRI images of Gd[DTPA]-encapsulated LTP and PLGA nanoparticles show a positive contrast increase with increasing concentration (Figure 1F,G). Additionally, the concentration-dependent increase is similar between both LTP and PLGA formulations. When compared to Gd[DTPA] standards (Figure 1E), the highest concentrations for LTP-Gd and PLGA-Gd (1.2 and 1.3 mg/mL, respectively) show intensities similar to the 0.1 mg/mL standard. This could be due to the polymer impeding water coordination with the Gd^{3+} chelate. Alternatively, the loading efficiency of Gd[DTPA] during nanoparticle synthesis, which was calculated to be ∼1% (w/w) (Supporting Information, Table 1), may be limiting the number of contrast agent molecules available for image enhancement.

Determining microglia cell viability after nanoparticle exposure is essential for potential use as a theranostic system. LTP nanoparticles have been shown to deliver plasmid DNA to human dermal fibroblasts with little to no cytotoxicity after an 11 day exposure.[26] Similarly, PLGA nanoparticles were used for nontoxic delivery of plasmid DNA to a variety of cell lines, including COS-7 and Cf2th, both frequently used for transfection.[59] After a 24 h exposure to both blank and drug-loaded LTP and PLGA nanoparticle formulations, both SIM-A9 and primary microglia showed 80−100% viability with all suspension concentrations ranging from 50 to 500 μg/mL (Figure 2A−D). Furthermore, the treatment of both SIM-A9 and primary microglia with blank LTP and PLGA nanoparticles showed no significant changes in metabolism when compared to that of PBS-treated cells (Figure 2E,F). An additional concern for the use of these particles in the brain is the potential for nanoparticle uptake to activate these cells. Microglial activation is accompanied by changes in cell morphology, cytokine release, and upregulation of phagocytosis and antigen presentation.[60−63] As evidenced by fluorescent imaging, exposure to either LTP or PLGA nanoparticles poses no morphological response in both SIM-A9 and primary microglia (Figure 3). This suggests that the uptake of our particles does not elicit an immune response typically associated with a change in cell shape. Moreover, nanoparticle uptake is exclusive to microglia even without surface modification with little to no particles seen to be associated with astrocytes. This poises microglia as an ideal target for enhanced contrast imaging with cellular resolution and further illustrates the benign nature of our nanoparticle formulations as potential delivery vehicles.

Microglia have a variety of receptors that trigger the phagocytic response, including TLRs (Toll-like receptors),[62] F_c receptors,[64] scavenger receptors,[65] and galectin-3/MAC-2[66] followed by the release of stimulatory molecules.[63] Analysis of our data suggests that neither LTP-Rol nor PLGA-Rol formulations alone induce substantial IL-1β, IL-6, or TNF-α release in SIM-A9 cells compared to LPS (Figure 4). In an attempt to suppress the inflammatory signaling cascade through PDE4 inhibition, LPS-stimulated cells were also cotreated with either LTP-Rol or PLGA-Rol nanoparticles (100 μg/mL for both). A slight decrease in TNF-α release was detected in cells cotreated with LTP-Rol and 100 ng/mL LPS, although not statistically significant. However, a significant decrease in TNF-α release was detected in cells treated with both 100 ng/mL LPS and PLGA-Rol nanoparticles. SIM-A9 cells cotreated with LTP-Rol and 100 ng/mL LPS also showed a significant decrease in IL-6 secretion compared to that with the 100 ng/mL LPS-only control. No difference in IL-6 secretion is seen between cotreatment with PLGA-Rol and LPS at 100 ng/mL versus control. It may be that longer treatment times or higher concentrations of the drug are necessary to completely block PDE4 activity and induce an anti-inflammatory state in these cells.

Recently, hydroxyl-terminated polyamidoamine (PAMAM) dendrimers were used as a backbone formulation for targeted delivery to mitochondria in glia under oxidative stress.[67] Triphenyl phosphonium (TPP) and N-acetyl cysteine (NAC) were conjugated to the dendrimer core by a GABA linker and used for mitochondrial targeting and delivery into activated microglia and macrophages. Moreover, this formulation was capable of passing through the blood−brain barrier.[68] Our

https://dx.doi.org/10.1021/acs.molpharmaceut.9b00489
Mol. Pharmaceutics 2020, 17, 1816−1826

nanoparticle formulations are readily and safely internalized by resting-state microglial cells without eliciting a proinflammatory immune response. Additionally, microglia were able to internalize our nanoparticles with higher efficiency than astrocytes, illustrating the potential for diagnostic imaging with cellular resolution. Although our current rolipram-loaded formulations were unable to suppress the release of inflammatory cytokines, we are poised to improve on this with further optimization of our synthesis parameters. Further investigation is planned to provide insight into the metabolic effects of our nanoparticle formulations and to confirm the bioavailability of the polymeric components in microglial cells after longer exposure times. The possibility of incorporation of these newly developed targeting systems with our nanoparticle formulations will enrich the growing number of potential theranostic candidates in this expanding field.

CONCLUSIONS

In this study, we compare the potential for LTP to the well-studied polymer PLGA as nanoparticle delivery systems of theranostic agents in microglia. LTP nanoparticles encapsulating either rolipram or Gd[DTPA] were characterized to be approximately 200−300 nm in size with high, negative ζ-potential values, indicating an anionic surface and low aggregation tendency. The loading efficiency of both PLGA and LTP nanoparticles with Gd[DTPA] was calculated to approximately 1%, a promising start for MRI contrast enhancement. All formulations (blank and loaded PLGA and LTP) were shown to be nontoxic to microglial cells, and preferential uptake of our nanoparticles was shown by microglia over astrocytes in mixed glial cultures. Rolipram-encapsulated nanoparticles did not induce an inflammatory response but were also unable to suppress the release of inflammatory cytokines over a 24 h period. Nonetheless, our nanoparticles pose an advancement toward diagnosing and treating neuroinflammation and provide a foundation for future investigation and optimization.

ASSOCIATED CONTENT

Supporting Information

The Supporting Information is available free of charge at https://pubs.acs.org/doi/10.1021/acs.molpharmaceut.9b00489.

Size distribution and ζ-potential graphs for additional formulations, loading efficiency standard curve, loading efficiency table, enzyme-linked immunosorbent assay (ELISA) standard curve for the cytokine multiplex assay using 4PL regression, and preferential uptake of nanoparticles by microglia in mixed glial cultures (PDF)

AUTHOR INFORMATION

Corresponding Authors

Yang H. Yun − *Department of Biomedical Engineering, Olson Research Center, University of Akron, Akron, Ohio 44325, United States;* orcid.org/0000-0001-5447-8833; Phone: 330-972-6619; Email: yy@uakron.edu; Fax: 330-374-8834

Leah P. Shriver − *Department of Chemistry, Knight Chemical Laboratories, University of Akron, Akron, Ohio 44325, United States*; Phone: 330-972-6940; Email: lshriver@uakron.edu; Fax: 330-972-6085

Authors

Celina Cahalane − *Department of Chemistry, Knight Chemical Laboratories, University of Akron, Akron, Ohio 44325, United States;* orcid.org/0000-0001-6722-6977

Jason Bonezzi − *Department of Chemistry, Knight Chemical Laboratories, University of Akron, Akron, Ohio 44325, United States*

John Shelestak − *Department of Biological Sciences, Kent State University, Kent, Ohio 44242, United States*

Robert Clements − *Department of Biological Sciences, Kent State University, Kent, Ohio 44242, United States*

Aliaksei Boika − *Department of Chemistry, Knight Chemical Laboratories, University of Akron, Akron, Ohio 44325, United States;* orcid.org/0000-0001-8249-0741

Complete contact information is available at: https://pubs.acs.org/10.1021/acs.molpharmaceut.9b00489

Author Contributions

C.C. performed in vitro experiments and data analysis; A.B. and J.B. did dynamic light scattering; R.C. and J.S. performed phantom MRI; L.P.S. and Y.H.Y. designed the study. The manuscript was written through contributions of all authors.

Notes

The authors declare no competing financial interest.

ACKNOWLEDGMENTS

The authors would like to thank Dr. Michael Konopka from the University of Akron Department of Chemistry for use of the confocal microscope for immunofluorescence imaging, Dr. Nick Leipzig from the University of Akron Department of Chemical and Biomedical Engineering for use of the multiplex for cytokine analysis, and GEOAnalytical for use of the ICP-OES for loading efficiency studies.

ABBREVIATIONS

BSA-FITC, bovine serum albumin-fluorescein isothiocyanate; CNS, central nervous system; ELISA, enzyme-linked immunosorbent assay; Gd, gadolinium; Gd[DTPA], gadolinium-diethylenetriaminepentaacetic acid; LTP, L-tyrosine polyphosphate; MRI, magnetic resonance imaging; PLGA, poly(lactic-*co*-glycolic) acid; TNF-α, tumor necrosis factor α

REFERENCES

(1) Li, W.; Viengkhou, B.; Denyer, G.; West, P. K.; Campbell, I. L.; Hofer, M. J. Microglia have a more extensive and divergent response to interferon-α compared with astrocytes. *Glia* **2018**, 2058.

(2) Carroll, J. A.; Race, B.; Williams, K.; Striebel, J.; Chesebro, B. Microglia Are Critical in Host Defense Against Prion Disease. *J. Virol.* **2018**, *92*, e00549−18.

(3) Michell-Robinson, M. A.; Touil, H.; Healy, L. M.; et al. Roles of microglia in brain development, tissue maintenance and repair. *Brain* **2015**, *138*, 1138−1159.

(4) Boddaert, J.; Bielen, K.; 's Jongers, B.; et al. CD8 signaling in microglia/macrophage M1 polarization in a rat model of cerebral ischemia. *PLoS One* **2018**, *13*, No. e0186937.

(5) Kim, M. E.; Park, P. R.; Na, J. Y.; Jung, I.; Cho, J. H.; Lee, J. S. Anti-neuroinflammatory effects of galangin in LPS-stimulated BV-2 microglia through regulation of IL-1β production and the NF-κB signaling pathways. *Mol. Cell Biochem.* **2018**, 451−452.

(6) Mancini, A.; Tantucci, M.; Mazzocchetti, P.; et al. Microglial activation and the nitric oxide/cGMP/PKG pathway underlie enhanced neuronal vulnerability to mitochondrial dysfunction in experimental multiple sclerosis. *Neurobiol. Dis.* **2018**, *113*, 97−108.

(7) Flygt, J.; Ruscher, K.; Norberg, A.; et al. Neutralization of Interleukin-1β following Diffuse Traumatic Brain Injury in the Mouse Attenuates the Loss of Mature Oligodendrocytes. *J. Neurotrauma* **2018**, 2837−2849.
(8) Taipa, R.; Ferreira, V.; Brochado, P.; et al. Inflammatory pathology markers (activated microglia and reactive astrocytes) in early and late onset Alzheimer disease: a *post mortem* study. *Neuropathol. Appl. Neurobiol.* **2018**, *44*, 298−313.
(9) Ponomarev, E. D.; Shriver, L. P.; Dittel, B. N. CD40 expression by microglial cells is required for their completion of a two-step activation process during central nervous system autoimmune inflammation. *J. Immunol.* **2006**, *176*, 1402−1410.
(10) Veremeyko, T.; Yung, A. W. Y.; Dukhinova, M.; et al. Cyclic AMP Pathway Suppress Autoimmune Neuroinflammation by Inhibiting Functions of Encephalitogenic CD4 T Cells and Enhancing M2 Macrophage Polarization at the Site of Inflammation. *Front. Immunol.* **2018**, *9*, 50.
(11) Neves-Zaph, S. R. *Phosphodiesterase Diversity and Signal Processing Within cAMP Signaling Networks*; Springer: Cham, 2017; pp 3−14.
(12) Omori, K.; Kotera, J. Overview of PDEs and Their Regulation. *Circ. Res.* **2007**, *100*, 309−327.
(13) Wilson, N. M.; Gurney, M. E.; Dietrich, W. D.; Atkins, C. M. Therapeutic benefits of phosphodiesterase 4B inhibition after traumatic brain injury. *PLoS One* **2017**, *12*, No. e0178013.
(14) You, T.; Cheng, Y.; Zhong, J.; et al. Roflupram, a Phosphodiesterase 4 Inhibitior, Suppresses Inflammasome Activation through Autophagy in Microglial Cells. *ACS Chem. Neurosci.* **2017**, *8*, 2381−2392.
(15) Cheng, H.; Wu, Z.; He, X.; et al. siRNA-mediated silencing of phosphodiesterase 4B expression affects the production of cytokines in endotoxin-stimulated primary cultured microglia. *Exp. Ther. Med.* **2016**, *12*, 2257−2264.
(16) Sommer, N.; Loschmann, P.; Northoff, G.; et al. The antidepressant rolipram suppresses cytokine production and prevents autoimmune encephalomyelitis. *Nat. Med.* **1995**, *1*, 244−248.
(17) Dyke, H. J.; Montana, J. G. The therapeutic potential of PDE4 inhibitors. *Expert Opin. Invest. Drugs* **1999**, *8*, 1301−1325.
(18) Grobner, T.; Prischl, F. C. Gadolinium and nephrogenic systemic fibrosis. *Kidney Int.* **2007**, *72*, 260−264.
(19) Prince, M. R.; Erel, H. E.; Lent, R. W.; et al. Gadodiamide administration causes spurious hypocalcemia. *Radiology* **2003**, *227*, 639−646.
(20) Filippi, M.; Rocca, M. A. MR Imaging of Multiple Sclerosis. *Radiology* **2011**, *259*, 659−681.
(21) Ratanajanchai, M.; Lee, D. H.; Sunintaboon, P.; Yang, S.-G. Photo-cured PMMA/PEI core/shell nanoparticles surface-modified with Gd−DTPA for T1 MR imaging. *J. Colloid Interface Sci.* **2014**, *415*, 70−76.
(22) You, Q.; Sun, Q.; Yu, M.; et al. BSA−Bioinspired Gadolinium Hybrid-Functionalized Hollow Gold Nanoshells for NIRF/PA/CT/MR Quadmodal Diagnostic Imaging-Guided Photothermal/Photodynamic Cancer Therapy. *ACS Appl. Mater. Interfaces* **2017**, *9*, 40017−40030.
(23) Wang, Z.; Carniato, F.; Xie, Y.; et al. High Relaxivity Gadolinium-Polydopamine Nanoparticles. *Small* **2017**, *13*, No. 1701830.
(24) Lux, F.; Sancey, L.; Bianchi, A.; Crémillieux, Y.; Roux, S.; Tillement, O. Gadolinium-based nanoparticles for theranostic MRI-radiosensitization. *Nanomedicine* **2015**, *10*, 1801−1815.
(25) Štefančíková, L.; Lacombe, S.; Salado, D.; et al. Effect of gadolinium-based nanoparticles on nuclear DNA damage and repair in glioblastoma tumor cells. *J. Nanobiotechnol.* **2016**, *14*, 63.
(26) Ditto, A. J.; Shah, P. N.; Gump, L. R.; Yun, Y. H. Nanospheres Formulated from l -Tyrosine Polyphosphate Exhibiting Sustained Release of Polyplexes and In Vitro Controlled Transfection Properties. *Mol. Pharm.* **2009**, *6*, 986−995.
(27) Ditto, A. J.; Shah, P. N.; Lopina, S. T.; Yun, Y. H. Nanospheres formulated from l-tyrosine polyphosphate as a potential intracellular delivery device. *Int. J. Pharm.* **2009**, *368*, 199−206.
(28) Cai, Q.; Shi, G.; Bei, J.; Wang, S. Enzymatic degradation behavior and mechanism of Poly(lactide-co-glycolide) foams by trypsin. *Biomaterials* **2003**, *24*, 629−638.
(29) Zweers, M. L. T.; Engbers, G. H. M.; Grijpma, D. W.; Feijen, J. In vitro degradation of nanoparticles prepared from polymers based on dl-lactide, glycolide and poly(ethylene oxide). *J. Controlled Release* **2004**, *100*, 347−356.
(30) Chen, X.; Ooi, C. P.; Lim, T. H. Effect of Ganciclovir on the Hydrolytic Degradation of Poly(lactide-co-glycolide) Microspheres. *J. Biomater. Appl.* **2006**, *20*, 287−302.
(31) Barcia, E.; Boeva, L.; García-García, L.; et al. Nanotechnology-based drug delivery of ropinirole for Parkinson's disease. *Drug Delivery* **2017**, *24*, 1112−1123.
(32) Rani, S.; Gothwal, A.; Pandey, P. K.; et al. HPMA-PLGA Based Nanoparticles for Effective In Vitro Delivery of Rifampicin. *Pharm. Res.* **2019**, *36*, No. 19.
(33) Ditto, A. J.; Reho, J. J.; Shah, K. N.; et al. In Vivo Gene Delivery with l -Tyrosine Polyphosphate Nanoparticles. *Mol. Pharm.* **2013**, *10*, 1836−1844.
(34) Gupta, A. Sen.; Lopina, S. T. Synthesis and characterization of L-tyrosine based novel polyphosphates for potential biomaterial applications. *Polymer* **2004**, 4653−4662.
(35) Ditto, A. J.; Shah, K. N.; Robishaw, N. K.; Panzner, M. J.; Youngs, W. J.; Yun, Y. H. The Interactions between l -Tyrosine Based Nanoparticles Decorated with Folic Acid and Cervical Cancer Cells under Physiological Flow. *Mol. Pharm.* **2012**, *9*, 3089−3098.
(36) Saura, J.; Tusell, J. M.; Serratosa, J. High-yield isolation of murine microglia by mild trypsinization. *Glia* **2003**, *44*, 183−189.
(37) Schneider, C. A.; Rasband, W. S.; Eliceiri, K. W. NIH Image to ImageJ: 25 years of image analysis. *Nat. Methods* **2012**, *9*, 671−675.
(38) Bligh, E. G.; Dyer, W. J. A Rapid Method of Total Lipid Extraction and Purification. *Can. J. Biochem. Physiol.* **1959**, *37*, 911−917.
(39) Abdi, H. The Bonferonni and Sidak Corrections for Multiple Comparisons, In *Encyclopedia of Measurements and Statistics*, In Saiki, N. J., Eds.; Sage: Thousan Oaks, CA, 2007; pp 103−107.
(40) Sen Gupta, A.; Lopina, S. T. Properties of l-tyrosine based polyphosphates pertinent to potential biomaterial applications. *Polymer* **2005**, *46*, 2133−2140.
(41) Sharma, S.; Parmar, A.; Kori, S.; Sandhir, R. PLGA-based nanoparticles: A new paradigm in biomedical applications. *Trends Anal. Chem.* **2016**, *80*, 30−40.
(42) Böstman, O.; Hirvensalo, E.; Mäkinen, J.; Rokkanen, P. Foreign-body reactions to fracture fixation implants of biodegradable synthetic polymers. *J. Bone Joint Surg.* **1990**, *72*, 592−596.
(43) Boche, D.; Perry, V. H.; Nicoll, J. A. R. Review: Activation patterns of microglia and their identification in the human brain. *Neuropathol. Appl. Neurobiol.* **2013**, *39*, 3−18.
(44) Valentini, X.; Deneufbourg, P.; Paci, P.; et al. Morphological alterations induced by the exposure to TiO2 nanoparticles in primary cortical neuron cultures and in the brain of rats. *Toxicol. Rep.* **2018**, *5*, 878−889.
(45) Lee, S. C.; Liu, W.; Dickson, D. W.; Brosnan, C. F.; Berman, J. W. Cytokine production by human fetal microglia and astrocytes. Differential induction by lipopolysaccharide and IL-1 beta. *J. Immunol.* **1993**, *150*, 2659−2667.
(46) Tracey, M. D. K. J.; Cerami, D. A., Ph. TUMOR NECROSIS FACTOR: A Pleiotropic Cytokine and Therapuetic Target. *Annu. Rev. Med.* **1994**, *45*, 491−503.
(47) Solé-Domènech, S.; Cruz, D. L.; Capetillo-Zarate, E.; Maxfield, F. R. The endocytic pathway in microglia during health, aging and Alzheimer's disease. *Ageing Res. Rev.* **2016**, *32*, 89−103.
(48) Destache, C. J.; Belgum, T.; Christensen, K.; Shibata, A.; Sharma, A.; Dash, A. Combination antiretroviral drugs in PLGA nanoparticle for HIV-1. *BMC Infect. Dis.* **2009**, *9*, 198.
(49) Maxfield, F. R.; McGraw, T. E. Endocytic recycling. *Nat. Rev. Mol. Cell Biol.* **2004**, *5*, 121−132.

https://dx.doi.org/10.1021/acs.molpharmaceut.9b00489
Mol. Pharmaceutics 2020, 17, 1816−1826

(50) McMahon, H. T.; Boucrot, E. Molecular mechanism and physiological functions of clathrin-mediated endocytosis. *Nat. Rev. Mol. Cell Biol.* **2011**, *12*, 517−533.
(51) Hewlett, L. J.; Prescott, A. R.; Watts, C. The coated pit and macropinocytic pathways serve distinct endosome populations. *J. Cell Biol.* **1994**, *124*, 689−703.
(52) Lim, J. P.; Gleeson, P. A. Macropinocytosis: an endocytic pathway for internalising large gulps. *Immunol. Cell Biol.* **2011**, *89*, 836−843.
(53) Hans, M.; Lowman, A. Biodegradable nanoparticles for drug delivery and targeting. *Curr. Opin. Solid State Mater. Sci.* **2002**, *6*, 319−327.
(54) Pate, K.; Safier, P.Chemical metrology methods for CMP quality. *Adv. Chem. Mech. Plan.***2016**:299−325 DOI: 10.1016/B978-0-08-100165-3.00012-7.
(55) Clogston, J. D.; Patri, A. K. *Zeta Potential Measurement*; Humana Press: 2011; pp 63−70.
(56) Lelyveld, V. S.; Atanasijevic, T.; Jasanoff, A. Challenges for Molecular Neuroimaging with MRI. *Int. J. Imaging Syst. Technol.* **2010**, *20*, 71−79.
(57) Laurent, S.; Elst, L. Vander.; Muller, R. N. Comparative study of the physicochemical properties of six clinical low molecular weight gadolinium contrast agents. *Contrast Media Mol. Imaging* **2006**, *1*, 128−137.
(58) Aime, S.; Cabella, C.; Colombatto, S.; Geninatti Crich, S.; Gianolio, E.; Maggioni, F. Insights into the use of paramagnetic Gd(III) complexes in MR-molecular imaging investigations. *J. Magn. Reson. Imaging* **2002**, *16*, 394−406.
(59) Koby, G.; Ofra, B.; Dganit, D.; Marcelle, M. Poly(D,L-lactide-co-glycolide acid) nanoparticles for DNA delivery: Waiving preparation complexity and increasing efficiency. *Biopolymers* **2007**, *85*, 379−391.
(60) Kreutzberg, G. W. Microglia: a sensor for pathological events in the CNS. *Trends Neurosci.* **1996**, *19*, 312−318.
(61) Cartier, N.; Lewis, C.-A.; Zhang, R.; Rossi, F. M. V. The role of microglia in human disease: therapeutic tool or target? *Acta Neuropathol.* **2014**, *128*, 363−380.
(62) Hanke, M. L.; Kielian, T. Toll-like receptors in health and disease in the brain: mechanisms and therapeutic potential. *Clin. Sci.* **2011**, *121*, 367−387.
(63) Fu, R.; Shen, Q.; Xu, P.; Luo, J. J.; Tang, Y. Phagocytosis of microglia in the central nervous system diseases. *Mol. Neurobiol.* **2014**, *49*, 1422−1434.
(64) Okun, E.; Mattson, M. P.; Arumugam, T. V. Involvement of Fc receptors in disorders of the central nervous system. *Neuromol. Med.* **2010**, *12*, 164−178.
(65) Husemann, J.; Loike, J. D.; Anankov, R.; Febbraio, M.; Silverstein, S. C. Scavenger receptors in neurobiology and neuropathology: Their role on microglia and other cells of the nervous system. *Glia* **2002**, *40*, 195−205.
(66) Rotshenker, S. The Role of Galectin-3/MAC-2 in the Activation of the Innate-Immune Function of Phagocytosis in Microglia in Injury and Disease. *J. Mol. Neurosci.* **2009**, *39*, 99−103.
(67) Sharma, A.; Liaw, K.; Sharma, R.; Zhang, Z.; Kannan, S.; Kannan, R. M. Targeting Mitochondrial Dysfunction and Oxidative Stress in Activated Microglia using Dendrimer-Based Therapeutics. *Theranostics* **2018**, *8*, 5529−5547.
(68) Teleanu, D.; Chircov, C.; Grumezescu, A.; et al. Blood-Brain Delivery Methods Using Nanotechnology. *Pharmaceutics* **2018**, *10*, 269.

https://dx.doi.org/10.1021/acs.molpharmaceut.9b00489
Mol. Pharmaceutics 2020, 17, 1816−1826